Mechanical Systems and Signal Processing 205 (2023) 110881

Contents lists available at ScienceDirect

Mechanical Systems and Signal Processing

journal homepage: www.elsevier.com/locate/ymssp

Frequency domain analyses of low-velocity impact loading of elastomeric foams

Somer Nacy [a], Behrad Koohbor [b], George Youssef [c,*]

[a] Department of Biomedical Engineering, University of Baghdad, Jaderyia, Baghdad 10071, Iraq
[b] Department of Mechanical Engineering, Rowan University, Glassboro, NJ 08028, USA
[c] Experimental Mechanics Laboratory, Mechanical Engineering Department, San Diego State University, San Diego 92182, USA

ARTICLE INFO

Keywords:
Impact loading
Frequency analysis
Polyurea
Elastomeric foams

ABSTRACT

Frequency analyses can reveal spectral features otherwise concealed within the time domain data. Such analyses are imperative to gain more insights into the undergoing dynamics in structures and materials, especially those with strong time dependence, such as elastomeric foams. This study aims to extend the applicability to data analysis from low-velocity impact scenarios by transforming into the frequency-domain, concurrently reporting crucial attributes of the dynamic loading and materials properties. Elastomeric polyurea foams with different densities were impacted at four different energies, ranging from 1.71 J to 7.09 J, to simulate low-velocity impact scenarios relevant to dynamic loading at different strain rates. In each impact test, a flattop drop mass was released from a preset height to control the impact velocity and energy while recording the impact and transmitted forces using impactor-mounted and base-mounted force sensors. The time-domain data of the primary impact was transformed into the frequency-domain using fast Fourier analysis. In the transformed domain, impact scenario characteristics, including acceleration and strain rate, and viscoelastic properties, *i.e.*, storage and loss moduli, were extracted and benchmarked to time domain results. The impact characteristics agreed with previous reports based on time domain analysis while revealing the frequency-dependence of the acceleration and strain rate on the foam density and impact energy. The extracted viscoelastic properties were also in reasonable agreement with previously reported properties while consistent with linear viscoelastic principles. The robustness of the demonstrated method unlocks the potential for more in-depth data analysis from other dynamic mechanical experimental setups, including high-velocity impact and shock loading.

1. Introduction

The novelty in experimental solid mechanics can be summed into contributions to new material systems, the development of innovative experimental techniques, or the application of novel and rigorous analysis approaches to revisit a well-studied problem. While these contributions are not necessarily mutually exclusive, they are commonly done independently due to the respective associated complexity. For example, the recent emergence of elastomeric foams to mitigate low-velocity impacts begs for more insightful analyses than those usually performed in the time domain [1,2]. In the latter, the analysis is limited to comparing the

* Corresponding author.
E-mail address: gyoussef@sdsu.edu (G. Youssef).

https://doi.org/10.1016/j.ymssp.2023.110881
Received 10 June 2023; Received in revised form 16 October 2023; Accepted 19 October 2023
Available online 25 October 2023

changes in the pulse characteristics, including the evolution in the amplitude and pulse width as standard performance metrics of the investigated materials in such loading scenarios. However, it is well known that such time domain signals conceal essential information about the material and its response to the incoming impact event. Revealing such significant material attributes can be exploited using frequency-domain analyses. This existing gap in the scientific literature, *i.e.*, the application of spectral analysis to low-velocity impacts of elastomeric foams, constitutes the primary motivation and novelty of the current study.

In dynamic testing of materials, regardless of the class or the strain rate, the time-domain signals recorded during the loading scenarios are encoded with convoluted mechanistic information but are usually exploited limitedly. The convoluted data is ubiquitous in all dynamic loading experiments, extending from the drop-weight tower, with strain rates of 100–1000 s^{-1}, to the plate impact setup at ultrahigh strain rates exceeding 10^7 s^{-1} [3,4]. For example, in low-velocity impacts conducted using drop-weight towers, the force–time histories are used to compare the response of a bare object to that covered by protective padding [5]. Here, a comparative emphasis is usually afforded to the changes in the peak amplitude and temporal attributes of the force pulse [5]. Moreover, the force–time histories have been used to forecast the strain history and strain rates based on an energy balance between the strain energy within the sample and the energy of the incoming impactor. Comparing the deformation to the damaged tested samples, reasonable agreements were previously reported [6]. On the other hand, in ultrahigh strain testing, the strain histories are analyzed, again temporally, to ensure dynamic equilibrium during loading and the strain rate calculation based on the primary rise time [7,8]. In the time domain analyses, the material properties (*e.g.*, elastic modulus) must be known *a priori* since the analysis relies on preconceived presumptions of the behavior of the materials to construct the dynamic stress–strain response. Leveraging the direct measurement of spatiotemporal strain, strain rate, and acceleration fields by image-based techniques (*e.g.*, digital image correlation), reconstruction of non-parametric stress–strain curves has been achieved for low impedance foams [9–14]. However, such image-based techniques require ultrahigh-speed cameras with limited spatial resolution and record time; therefore, they are economically inconvenient solutions. It is imperative to reiterate that despite its apparent shortcomings, time domain analysis remains the standard approach in analyzing the data in many dynamic experiments, arguably rightfully so (*e.g.*, [15]). However, as discussed next, spectral analysis can elucidate more mechanistic insights otherwise concealed within the temporal signals.

The time domain signals can be explored and exploited in the frequency-domain to extract concealed spectral features. At the onset, it is worth noting that frequency-domain analyses are the standard in vibration and structural studies [16,17]; however, to a lesser extent, in the mechanics of low-velocity impacts. For example, Li *et al.* applied frequency-domain analysis to temporal data from the low-velocity impact of high-porosity closed-cell aluminum foams but limited the focus of the frequency analysis to assessing the errors associated with sensor spectral characteristics [18]. Similarly, Found *et al.* transformed the time-domain data of low-velocity, low-energy impacts ($<$1.5 J) to the frequency-domain to determine the cutoff filtering frequency to clean the experimental data before further processing [19]. They also affirmed that the filtering cutoff frequency is not associated with the dynamics of carbon fiber-reinforced polymer composite panels [19], which they deemed consistent with previous investigations [20–22]. Sun and Gu studied the experimental data obtained from split Hopkinson bar testing of three-dimensional angle-interlock woven composites to discern the interrelationship between the gas pressure used to activate the striker bar with the energy distribution of the stress wave [23]. They found that the striker energy is concentrated in the low-frequency region ($\lesssim$8500 Hz) for different strike velocities, as far as the striker bar length was kept constant [23]. However, Sun and Gu did not attempt to extract material properties nor further analyze the impact characteristics in the frequency-domain, *i.e.*, the rest of their insightful analysis was done in the time domain. Another critical application of spectral analysis is the investigation of dynamic signatures due to acoustic emissions during the testing of brittle materials, *e.g.,* concrete-based structures or granular materials, due to the nucleation and propagation of internal and superficial cracks [24,25]. For example, Basavanna *et al.* leveraged the power of frequency analysis to qualitatively assess the damping differences between glass fiber-reinforced epoxy composites and reinforcing shape memory polymers using a network of piezoelectric sensors to capture and analyze the power spectrum signatures after low-velocity impacts [26]. Hoseinlaghab *et al.* investigated the mechanical response of glass fiber-reinforced composites using frequency analysis to detect and report dominant damage mechanisms during tensile loading by recording the emanating acoustic emission during testing [27]. In all, while the utility of spectral analyses was sporadically leveraged in the analysis of impact data, the results were focused on either elementary signal processing (*e.g.*, filtering) or basic dynamic assessment of experimental setups. Hence, the focus herein is on extending the applicability of spectral analysis to extract material properties from impact-loading scenarios.

The studies discussed above focus on the spectral investigation of the damage of composite panels or rigid materials with limited or superficial frequency-domain analysis of the impact force. However, the application of spectral analyses to highly deformable materials, *e.g.*, elastomeric foams, in low-velocity impacts has been absent from the open literature. Such loading scenarios are engulfed by nonlinear, reversible deformation and significant rebound, contrary to the impact of composite panels, for example. Therefore, the dynamic response of elastomeric foams due to low-velocity impacts can be analyzed for concurrently extracting impact characteristics and material properties when transformed in the frequency-domain. The emphasis on elastomeric foams stems from a twofold rationale. First, recent advances in manufacturing elastomeric foams from shock-tolerant and impact-resistant materials, *e.g.*, polyurea [1,2,28–32], positioned these materials as viable alternatives for mitigating biomechanical impacts common in individual and group sports. Second, the energy absorption performance of elastomeric foams was found to be comparable to their rigid counterpart in low-velocity and low-energy impacts [33]; however, the latter is not reusable due to the accumulation of internal damage in the cellular structure and the material entrapped in the cell walls [34]. Contrarily, elastomeric foams exhibit nonlinear deformation, improving energy absorption and dissipation due to the conversion of the impact energy into strain energy. The mechanical response of this class of materials is described as hyperelastic, *i.e.*, the large deformation is reversible [35]. In other words, elastomeric foams recover their original geometry after a short resting period, accumulating minimal internal damage over repeated impacts. The latter is also beneficial from protection and economic perspectives, where protective paddings or orthotics are expected to sustain their

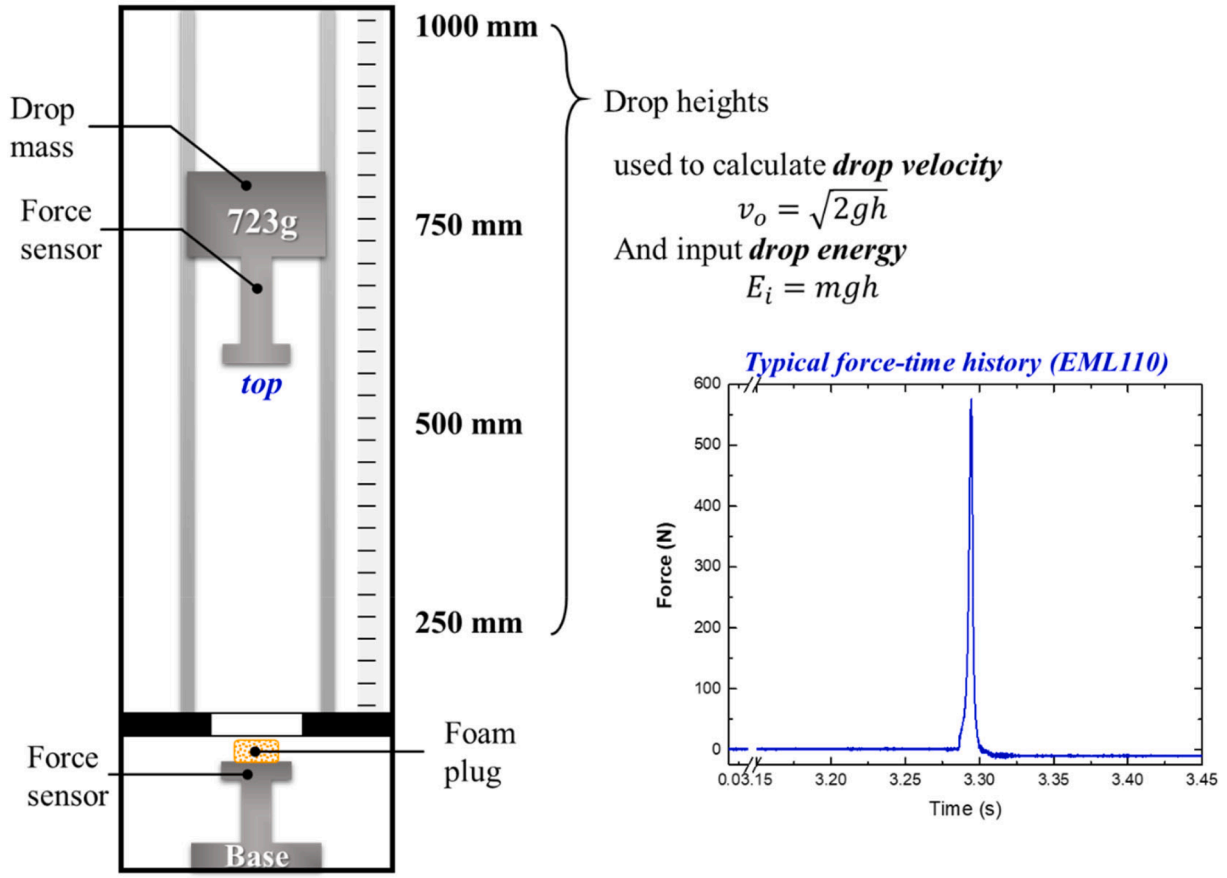

Fig. 1. . Schematic representation of the low-velocity impact experiment using a drop mass (m) at four different elevations (h); also includes a typical raw force–time history collected from impact at drop height of 250 mm.

performance even after frequent and repeated impacts [31,36].

This paper aims to exploit frequency-domain analyses to detect and report the dynamic signatures of elastomeric polyurea foams that underwent single impact events. Elastomeric polyurea foams were dynamically tested using a drop weight tower by releasing a predefined flat mass from different heights, submitting the foam samples to low-velocity impacts at energies ranging from 1.77 to 7.09 J. The novelty of the research leading to this publication lies in bridging the frequency and time domain analyses to elucidate the dynamic behavior of highly deformable cellular solids while concurrently extracting the dynamic material properties without resorting to any additional testing and costly imaging setups.

2. Materials and methods

Two density variations of elastomeric polyurea foams, $\rho_1 = 110\ \mathrm{kg.m^{-3}}$ (EML110) and $\rho_2 = 230\ \mathrm{kg.m^{-3}}$ (EML230), were fabricated by closely following the manufacturing process reported in [1,2]. In general, polyurea foams used in this study were produced by mechanically mixing oligomeric diamine (Versalink® P1000, AirProducts Inc. currently Evonik), diisocyanate (MPI-143L, Dow), and deionized water at specified ratios based on the dimensions of the mold cavity and foam rise rate [1,2]. The mixed foam slurry was then quickly transferred to a Teflon®-coated aluminum mold, where it was left to cure for 24 h at ambient conditions and then for an additional 48 h for dehydration. Cubic samples, with ~ 18 mm edge length, were extracted from the cured and dehydrated foam sheets using a die punch. The samples were submitted to a low-velocity impact scenario by releasing a 723 g mass (m) from a certain height, h, (ranging between 250 and 1000 mm, with 250 mm intervals) to control the imparted impact energy, *i.e.*, $E_i = mgh$. Irrespective of the foam density, each sample was impacted only once at each impact energy, including energies of 1.77 J, 3.55 J, 5.32 J, and 7.09 J. The impact force was collected using a sensor attached to the impactor head, while the transmitted force was acquired from another sensor attached to the base on which the foam sample was rested. The force–time histories were recorded at a sampling rate of 15 kS/s. Fig. 1 shows a schematic of the experimental setup, delineating the location of the top and bottom sensors with respect to the foam sample and the impactor head. The force–time histories were utilized in frequency-domain analyses, as discussed in the next section, while the time-domain analyses were reported elsewhere [32,37].

3. Frequency-domain analysis

As mentioned in the previous section, the impact and transmitted force–time histories were recorded using sensors positioned above and below the foam samples. The spectral analyses described below rely on first transforming these force–time histories into the frequency-domain using a fast Fourier transform. Overall, the frequency analyses were divided into two regimes, namely impact characteristics and material properties extraction. In the former, only the impact force recorded from the top sensor was used, while in the latter, the frequency-transformed impact and transmitted forces were used.

3.1. Spectral analysis for determination of impact characteristics

The raw impact force–time history, $f_i(t)$, was transformed into the frequency-domain using the discrete fast Fourier transform, such that

$$F_i(\omega) = \sum_{n=0}^{N-1} (f_i)_n e^{\frac{-i\omega n}{N}} \tag{1}$$

where, F_i is the transformed impact force, ω is the circular frequency, and N is the number of points recorded in the time-domain. In other words, the spectral transformation was done in MATLAB® using discrete Fourier transform, performed on the raw data without any pre-processing steps. Here, the focus is on the magnitude of F_i to calculate the acceleration, $a(\omega)$, velocity, $v(\omega)$, and displacement, $\delta(\omega)$, in the frequency-domain using,

$$a(\omega) = |F_i(\omega)|/m \tag{2}$$

$$v(\omega) = \frac{a(\omega)}{i\omega} + v_o \tag{3}$$

$$\delta(\omega) = -a(\omega)/\omega^2 \tag{4}$$

where, m is the mass of the drop impactor (taken to be 723 g for the current experiment), and v_o is the initial velocity due to the drop height ($v_o = \sqrt{2gh}$, g is the gravitation acceleration) such that the drop height (h) ranged from 250 to 1000 mm to adjust the impact energy, as discussed in the previous section.

In the frequency-domain, the spectral features have been decomposed as a function of frequency, allowing the calculation of the strain rate, $\dot{\varepsilon}$, from the spectral velocity (Eq. (3)),

$$\dot{\varepsilon}(\omega) = \frac{v(\omega)}{l_o} \tag{5}$$

based on the original length of the sample (l_o). Similarly, the engineering strain can be calculated by dividing the spectral displacement (Eq. (4)) by the original length,

$$\varepsilon(\omega) = \frac{\delta(\omega)}{l_o} \tag{6}$$

3.2. Spectral analysis for extraction of material properties

A unique characteristic of the experimental protocol undertaken in this study is the concurrent recording of the impact and transmitted force–time histories due to the release of the drop mass in this low-velocity impact scenario. In other words, the interactions of the forces with the sample constitute the true dynamics of the material by considering the impact force (imparted from the drop mass and recorded by the top sensor) as the input force while the transmitted force (recorded by the bottom sensor) is the output force since the impact must have trespassed the sample before arriving to the recording site. Such input/output relationship is represented in the frequency-domain in terms of the experimental transfer function, $TF_{exp}(\omega)$, by dividing the frequency spectrum of the transmitted force, $F_t(\omega)$, by the frequency spectrum of the impact force,

$$TF_{exp}(\omega) = \frac{F_t(\omega)}{F_i(\omega)} \tag{7}$$

On the other hand, the theoretical transfer function can be derived by considering the representative model in Appendix A, where dividing the expression of the output force by that of the input force yields,

$$TF_{th}(\omega) = \frac{ka + c^2\omega^2}{a^2 + c^2\omega^2} + i\frac{ac\omega - kc\omega}{a^2 + c^2\omega^2} \tag{8}$$

where, k is the foam stiffness, c is the dampening coefficient of the foam, and $a = k - m\omega^2$ with m being the drop mass. It is imperative to note that the calculated stiffness and dampening are functions of the frequency at which they were extracted. The values of the stiffness and dampening can then be calculated from,

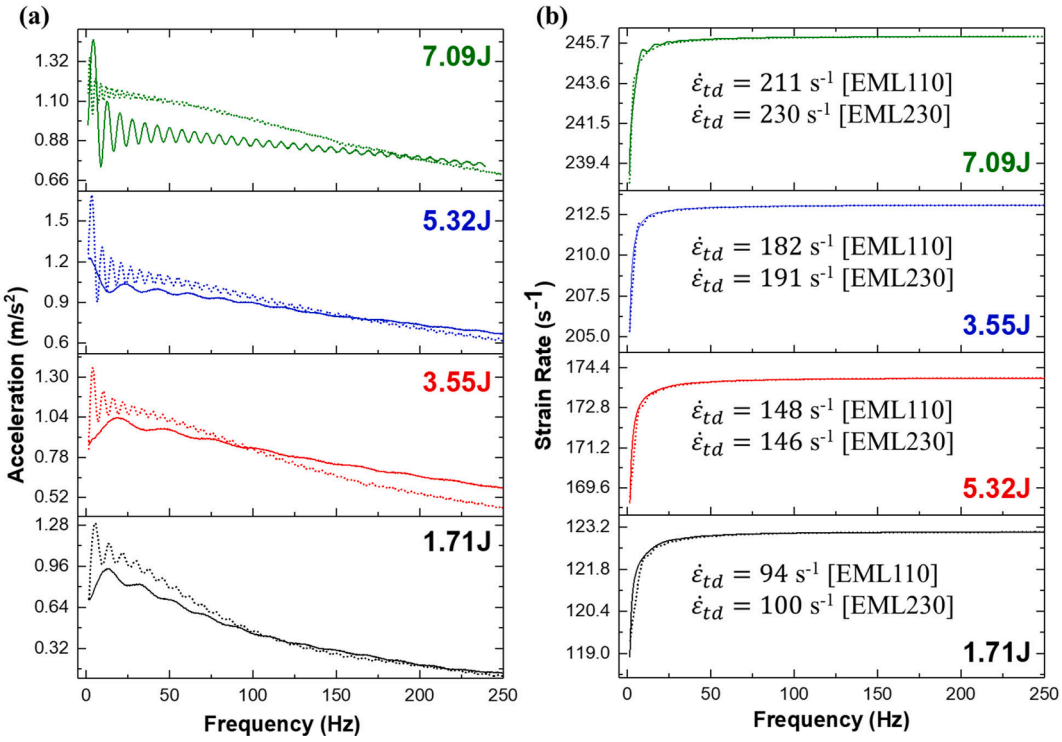

Fig. 2. . Spectral results of (a) acceleration and (b) strain rate as a function of impact energy ranging from 1.71 J to 7.09 J for polyurea foams with densities 110 kg/m^3 (solid lines) and 230 kg/m^3 (dotted lines). The strain rate from previous time-domain (TD) analysis are also listed in (b) [6].

$$\left|TF_{exp}\right| - \left|TF_{th}\right| = 0 \tag{9a}$$

$$arg\left(TF_{exp}\right) - arg\left(TF_{th}\right) = 0 \tag{9b}$$

as a function of frequency by extending the frequency-stiffness and frequency-dampening relationships at resonance. The stiffness-frequency relationship is $\omega_p = \sqrt{\frac{k}{m}}$ and critical damping-frequency relationship is $c_c = 2m\omega_p$. It then follows that the damping ratio as a function of frequency, $\zeta = \frac{c}{c_c}$, leading to the quality factor, $Q = 1/2\zeta$. The latter is a measure of the ratio between stored and dissipated energy per each cycle. Similarly, the storage modulus can be calculated from the simplified definition of stiffness, $E' = \frac{kl_o}{A}$, where A is the cross-sectional area of the foam sample. The loss modulus is defined as $E'' = \frac{cv_i\omega}{A\varepsilon}$. Finally, the transmissibility of a force through the foam, *i.e.*, a measure of the ratio between the transmitted and impact forces, could be calculated from the magnitude of the transfer function in the frequency-domain, a topic for future research.

4. Results and discussion

This section is divided into two subsections analogous to the structure of § 3, where the frequency decomposition of the impact input force is first used to calculate the impact characteristics. The results of the material properties extraction from the frequency-domain data of the impact and transmitted forces are presented in the second subsection.

4.1. Impact characteristics

Since the acceleration is linearly related to the force, the frequency spectrum of only the former is discussed in lieu of the latter for brevity while noting that the force-frequency plots can be easily attained by multiplying the acceleration by the drop mass. The strain rate spectra are only plotted instead of the velocity using a similar rationale. The remaining attributes, *i.e.*, displacement and strain, can be readily extracted using Eqs. (4) and (6), respectively. Fig. 2a plots the acceleration spectra based on the frequency decomposition of the force–time history of low-velocity impacts at four different drop heights, while Fig. 2b shows the corresponding strain rate dependence on frequency for the same impact conditions.

The acceleration spectra (Fig. 2a) yield three noteworthy observations commonly concealed within the time-domain data. First, the acceleration decays as the frequency increases from DC to ~ 250 Hz, irrespective of the foam density, generally indicating higher contributions of the acceleration (and, in turn, the force) at lower frequencies. The higher contributions in the low-frequency regime

are associated with the viscoelastic properties of elastomeric foams, where the stiffness values follow a similar behavior, increasing as a function of frequency, as discussed in the forthcoming sections. The change in stiffness gives rise to frequency-based evolution in resistance to deformation, where the foam is more compliant at low-frequency, contributing to larger deformations and higher dissipated strain energy [35]. The dc-acceleration values for EML110 (*i.e.*, low-density polyurea foam) centered around 0.94 m/s^2 (ranging from 0.70 m/s^2 for drop energy of 1.71 J to 0.97 m/s^2 at the highest impact energy of 7.09 J). The dc-accelerations for EML230 fluctuated from 0.71 m/s^2 to 1.14 m/s^2 over the same energy range. Thus, the DC-acceleration values show interdependence on the drop energy and foam density. Notably, the spectral acceleration decay does not reach zero, implying the impact mitigation efficacy of polyurea foams at higher impact frequencies, *i.e.*, the spectral response did not bottom-down and can potentially sustain moderate velocity impacts. The terminal acceleration values, taken at the cutoff frequency (*i.e.*, ~250 Hz or where the curve stopped), for EML110 are *ca.* 0.13 m/s^2, 0.58 m/s^2, 0.66 m/s^2, and 0.74 m/s^2 when impacted at 1.71 J, 3.55 J, 5.32 J, and 7.09 J, respectively. The corresponding terminal values for EML230 foam samples are 0.10 m/s^2, 0.45 m/s^2, 0.61 m/s^2, and 0.69 m/s^2 for the same impact energies. Like the dc counterparts, terminal accelerations also exhibit interdependence on the density and the impact intensity. In general, the energy-acceleration relationship is intuitive from an elementary mechanics point of view; however, the role of the foam density in altering the acceleration points to the difference in the amount of base material entrapped in the spheroidal cell walls. For example, the acceleration changes in the high-density foam demonstrate the full participation of the microcellular structure and the material entrapped within, *i.e.*, the severity of the impact is resisted by cumulative contributions of the structure and the material. The acceleration also influences the inertial stress developed in the foam plug as a function of sample length, strain rate, and the rate of strain rate, as previously shown in [38].

Second is the reverberations in the acceleration spectra, superimposed on the moving mean of the data as the energy increases regardless of the foam density. The reverberations are ubiquitous at the high impact energy in the low-density foam variant and all acceleration spectra of the high-density foam, irrespective of the impact energy. While these reverberations are with damped attributes at higher frequencies, their existence is intriguing. The reverberations dampen faster in the high-density foams than in their low-density counterparts. The spectra response of EML230 at frequencies $>$ 100 Hz are nearly free of reverberations, indicating higher dampening attributes due to the entrapment of higher base material content in the microcellular peripheries. In other words, the nature of low-velocity impacts leverages the collective dampening performance of the foam, including the cell deformation, viscoelastic properties of the base polymer, and even the contribution of the slow escaping of air within the microcellular structure. The spectral reverberations are thought to be associated with the change in the stiffness, which coincides with the presence of the reverberations in all the acceleration spectra of EML230 since higher foam density translates to enhanced stiffness. Gibson and Ashby demonstrated that the foam elastic modulus (a measure of the cellular structure stiffness) is directly proportional to the elastic modulus of the based material and the squared ratio between the foam density and the density of the base material [33]. Another possible source is the size distribution of the microcellular structure that gives rise to acceleration bursts at specific frequencies as enough energy is accumulated during the imposition of the impact loading. The reverberations are also attributed to the constant deformation rate, as discussed below.

The final observation based on the acceleration spectra shown in Fig. 2a is the crossover frequency between spectra of EML110 and EML230. The crossover frequency is taken to be the spectral intersection between the response of the low- and high-density foams, *i.e.*, the frequency corresponding to $a(\omega)_{EML110} - a(\omega)_{EML230} \approx 0$. The crossover frequencies are 114 Hz, 98 Hz, 167 Hz, and 194 Hz for impacts at 1.71 J, 3.55 J, 5.32 J, and 7.09 J, respectively. The spectra of both foams nearly overlap after the crossover frequency for the lowest impact scenario at an energy of 1.71 J (Fig. 2a bottom panel). Alternatively, the acceleration spectra depart from each other after the crossover frequency for all other impact energies, where acceleration components of EML110 rise above those of EML230 despite the opposite before the crossover. The crossover frequency indicates a property-matching point where the performance of the investigated foams is identical regardless of the density. At the crossover, the convoluted contributions of the cellular structure (shape, size, and distribution) and viscoelastic properties of the base materials converge to sustain the impact imposition at this frequency, showing indifference to the foam density. Notably, the crossover frequency shifts to higher frequencies as the impact energy increases, indicating the activation of the responsible deformation mechanisms occurring at earlier impact times since the deformation rate ascends as the impact energy increases.

Fig. 2b plots the strain rate as a function of frequency for EML110 and EML230 at all four impact energies. The figure also reports the peak strain rates for each impact scenario, extracted from the time-domain data based on digital image correlation analyses of high-speed photographs of the same impact events conducted in a previous study [37]. The strain rates from the time-domain and frequency-domain are in reasonable agreement. The spectral strain rates generally show independence on the foam density since the base material is the same in both cases, where the viscoelastic properties dominate the response. However, after a sharp increase in the strain rate in the low-frequency regime ($<$50 Hz), the strain rates reach frequency-independent values of 123 s^{-1}, 174 s^{-1}, 213 s^{-1}, and 246 s^{-1} (calculated average over 50 Hz to terminal frequency) for impact scenarios at 1.71 J, 3.55 J, 5.32 J, and 7.09 J, respectively. The initial frequency-dependence of the strain rate is attributed to the slowing down of the impactor head as the impact time increases, achieving higher levels of engagement of the entrapped material and leading to the temporal force peak in the time domain. On the other hand, the frequency-independent strain rates at higher frequencies ($>$50 Hz) are associated with invariant deformation mechanisms due to the constant initial velocity upon impact. The interrelationship between the strain rate and the frequency gives rise to the strain rate sensitivity of elastomeric polyurea foams, as recently discussed by Koohbor *et al.* [37].

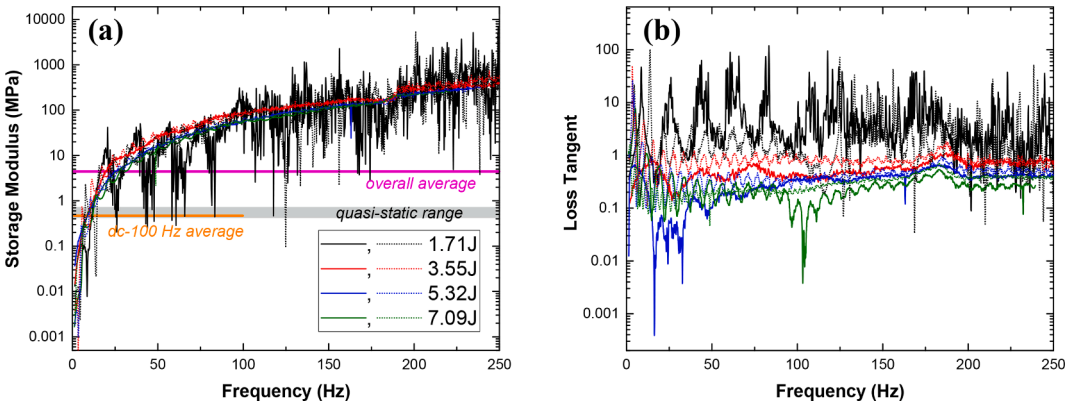

Fig. 3. . Extracted viscoelastic properties of polyurea foams (solid lines for EML110 and dotted lines for EML230) from frequency analysis of low velocity impacts, including (a) storage modulus and (b) loss tangent ($\tan\delta = E'/E''$).

4.2. Material characteristics

Fig. 3 plots the viscoelastic properties of polyurea foams with two densities (110 and 230 kg/m^3) based on frequency-domain analysis of low-velocity impact scenarios at impact energies ranging from 1.71 J to 7.09 J. The viscoelastic properties were calculated using the transfer function approach discussed in the previous section, leveraging the simultaneous recording of the impact (input) and transmitted (output) force–time histories. Fig. 3a reports the storage modulus as a function of frequency from DC to ~ 250 Hz, while Fig. 3b depicts the loss tangent over the same frequency range. Fig. 3b is calculated by dividing the storage modulus (Fig. 3**a**) by the loss modulus (calculated based on the damping coefficient, impact velocity, frequency, cross-sectional area, and strain rate). This section emphasized the viscoelastic properties (*i.e.*, storage modulus and loss tangent) since the remaining material parameters discussed in Section 3.2 are readily relatable.

The reported storage modulus in Fig. 3a can be summarized into three observations. First, the storage modulus is independent of the foam density and impact energy, where the moduli (on average) lay on top of one another (*i.e.*, the lines are nearly indistinguishable). The storage modulus ranges from ~ 10 kPa at low frequency to ~ 300 MPa at the terminal frequency (*i.e.*, ~250 Hz). The independence of the storage modulus from density and energy implies that the demonstrated frequency-domain analysis method from the impact and transmitted force–time histories can resolve the viscoelastic properties of the base material (polyurea), including the microcellular structural effects. While this observation may appear counterintuitive since the foam modulus is generally known to be proportional to the squared density, as discussed above and initially reported in [33], the results are consistent with the analysis approach demonstrated herein. Since the storage modulus was calculated based on the transfer function concept, *i.e.*, dividing the spectral output function by the spectral input function, it suppressed the contributions of the impacting conditions. The division of the force-frequency spectra results in filtering the testing conditions (*e.g.*, cancels the impact mass and impacting velocity effects) while giving rise to the base material properties and influence of the spheroid cell geometry.

Second, the average storage moduli (Fig. 3a) agreed with previous reports in the literature. The overall average of the storage moduli is 3.48 MPa for EML110 and 3.96 MPa for EML230, while at the low-frequency regime, (<100 Hz) averages are 390 kPa and 446 kPa, respectively. The low-frequency average modulus (aggregate of EML110 and EML230 moduli) is within the range of the quasi-static compressive elastic modulus values previously reported in [1]. Since the elastic and storage moduli are stiffness measures that dictate the resistance to deformation under load imposition, the comparison is justified, especially in the low-frequency regime. Such a qualitative agreement between the storage and the quasi-static moduli implies the applicability of the demonstrated analysis approach to extract meaningful viscoelastic properties from a simple low-velocity impact when treated in the frequency-domain. It is imperative to note that quantitative comparison is not possible within the realm of available data, which will be the focus of future research to avoid digression from the overall objective of this paper.

Finally, the storage moduli (Fig. 3a) for EML110 and EML230 impacted with 1.71 J exhibit superimposed oscillations throughout the investigated frequency range. Nonetheless, the moving average of these two curves still coincides with the moduli extracted from the remaining impact energies. These oscillations are considered experimental artifacts due to the sensitivity of the force sensors and the relatively low force amplitude (640 N for 1.71 J vs. 1721 N for 3.55 J) [6]. Such artifacts are absent from the storage moduli extracted from the transfer function of impact at 3.55 J, 5.32 J, and 7.09 J, affirming the hypothesis about their source.

The spectral loss tangent of EML110 and EML230 foams as a function of the impact energy is shown in Fig. 3b. The loss tangent is a measure of the dampening performance of viscoelastic material, showing, based on the results in Fig. 3b, a dependence on the impact energy. The spectral average of the loss tangent for the 1.71 J impact scenario is 8.58 for EML110 and 4.00 for EML230, making it the highest dampening performance of the investigated impacts. For the remaining cases, the loss tangent was below unity. The relatively high dampening at low-impact energy is responsible for the absence of reverberation in acceleration spectra, discussed in the previous section. Remarkably, the average spectral loss tangent for EML110 and EML230 is 0.32 when impacted at the highest energy of 7.09 J, justifying the prevalence of the reverberations in the former and their persistence in the latter. Overall, the viscoelastic properties

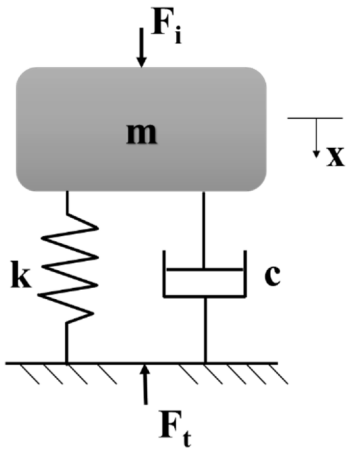

Fig. A1. . Simplified lumped mass model used in the derivation of the theoretical model.

stipulate the conditions for achieving the acceleration and strain rate results discussed in the previous section while demonstrating the impact mitigation efficacy of polyurea foams. The latter agrees with previous reports by the authors [37].

5. Conclusion

Time-domain data from the force sensors during the low-velocity impacts were transformed into the frequency-domain using the fast Fourier transform. The impact and transmitted force–time histories were collected upon releasing a flattop drop mass on polyurea foam plugs with different densities. The transformed data was exploited to extract impact and materials attributes, including acceleration, strain rate, and viscoelastic properties of the foam (*e.g.*, storage and loss moduli). The transformed acceleration elucidated the interdependence of the dynamics on the energy and foam density. At the same time, the spectral strain rate was only dependent on the impact energy but insensitive to the density. In analyzing spectral acceleration, crossover frequency was introduced to demonstrate the correspondence of foam densities under a similar impact scenario, in which the foam plugs sustained impact imposition irrespective of the density. A unique byproduct of frequency analysis is the concurrent extraction of viscoelastic properties of the foam by leveraging the transformed data of the impact and transmitted force–time histories. The storage moduli, a measure of the resistance to deformation, were independent of impact energy since the base material in both foam density variants is the same, *i.e.*, polyurea. On the other hand, the loss tangent, a measure of energy dissipation, exhibited interdependence on the impact energy. In all, the demonstrated frequency analysis procedure can be applied to other dynamic experimental mechanics data, including high-velocity and shock-loading scenarios.

Declaration of Competing Interest

The authors declare that they have no known competing financial interests or personal relationships that could have appeared to influence the work reported in this paper.

Data availability

Data will be made available on request.

Acknowledgment

This material is based upon work supported by the National Science Foundation under Grant No. 2035663 (G.Y.) and Grant No. 2035660 (B.K.). The authors are also grateful for internal funding from San Diego State University and Rowan University.

Appendix

Theoretical transfer function

The theoretical transfer function of an impact scenario can be derived using a simple lumped mass model, showing in Fig. A1. The input force balance based on the forces in the mass, spring, and dashpot is,

$$F_i = m\ddot{x} + c\dot{x} + kx \tag{A.1}$$

The transmitted force balance is based on the stiffness and dampening of the foam, which can be represented as,

$$F_t = c\dot{x} + kx \tag{A.2}$$

Therefore, the theoretical transfer function can be calculated as the ratio between the transmitted (output) and impact (input) force balances,

$$TF_{th} = \frac{F_t}{F_i} = \frac{c\dot{x} + kx}{m\ddot{x} + c\dot{x} + kx} \tag{A.3}$$

However, the frequency transformed variable in A.1 and A.2 is,

$$X = xe^{i\omega t} \tag{A.4}$$

Hence, the transfer function can be presented in the frequency-domain as,

$$TF_{th}(\omega) = \frac{(i\omega c + k)x}{(-\omega^2 m + i\omega c + k)x} = \frac{k + i\omega c}{k - \omega^2 m + i\omega c} \tag{A.5}$$

The transfer function (A.5) is multiplied by the complex conjugate to obtain the complete representation in the frequency-domain, which is compared in the main manuscript to the time-domain response.

$$TF_{th}(\omega) = \frac{ka + c^2\omega^2}{a^2 + c^2\omega^2} + i\frac{ac\omega - kc\omega}{a^2 + c^2\omega^2}$$

where, $a = k - m\omega^2$.

References

[1] N. Reed, et al., Synthesis and characterization of elastomeric polyurea foam, J. Appl. Polym. Sci. 137 (26) (2020) 48839.
[2] Youssef, G. and N. Reed, *Scalable manufacturing method of property-tailorable polyurea foam.* 2021, Google Patents.
[3] J.E. Field, et al., Review of experimental techniques for high rate deformation and shock studies, Int. J. Impact Eng. 30 (7) (2004) 725–775.
[4] C.R. Siviour, J.L. Jordan, High strain rate mechanics of polymers: a review, J. Dynam. Behav. Mater. 2 (1) (2016) 15–32.
[5] F. Penta, et al., Low-velocity impacts on a polymeric foam for the passive safety improvement of sports fields: meshless approach and experimental validation, Appl. Sci. 8 (7) (2018) 1174.
[6] G. Youssef, et al., Density-Dependent Impact Resilience and Auxeticity of Elastomeric Polyurea Foams, Adv. Eng. Mater. 25 (1) (2023) 2200578.
[7] J. Liu, et al., Impact testing of polymeric foam using Hopkinson bars and digital image analysis, Polym. Test. 36 (2014) 101–109.
[8] B. Song, W. Chen, X. Jiang, Split Hopkinson pressure bar experiments on polymeric foams, Int. J. Veh. Des. 37 (2–3) (2005) 185–198.
[9] B. Koohbor, et al., Investigation of the dynamic stress–strain response of compressible polymeric foam using a non-parametric analysis, Int. J. Impact Eng. 91 (2016) 170–182.
[10] B. Koohbor, A. Kidane, W.-Y. Lu, Effect of specimen size, compressibility and inertia on the response of rigid polymer foams subjected to high velocity direct impact loading, Int. J. Impact Eng. 98 (2016) 62–74.
[11] S. Ravindran, et al., Experimental characterization of compaction wave propagation in cellular polymers, Int. J. Solids Struct. 139 (2018) 270–282.
[12] B. Koohbor, A. Kidane, W.-Y. Lu, Characterizing the constitutive response and energy absorption of rigid polymeric foams subjected to intermediate-velocity impact, Polym. Test. 54 (2016) 48–58.
[13] S. Koumlis, L. Lamberson, Strain rate dependent compressive response of open cell polyurethane foam, Exp. Mech. 59 (7) (2019) 1087–1103.
[14] F. Pierron, Addendum to 'characterising the strain and temperature fields in a surrogate bone material subject to power ultrasonic excitation', Strain 52 (3) (2016) 186–190.
[15] Standard, A., *ASTM D1621-16.* Standard test method for compressive properties of rigid cellular plastics, 2016.
[16] M. Mršnik, J. Slavič, M. Boltežar, Frequency-domain methods for a vibration-fatigue-life estimation–application to real data, Int. J. Fatigue 47 (2013) 8–17.
[17] M. Varanis, et al., MEMS accelerometers for mechanical vibrations analysis: A comprehensive review with applications, J. Braz. Soc. Mech. Sci. Eng. 40 (11) (2018) 1–18.
[18] B. Li, G. Zhao, T. Lu, Low strain rate compressive behavior of high porosity closed-cell aluminum foams, Sci. China Technol. Sci. 55 (2) (2012) 451–463.
[19] M. Found, I. Howard, A. Paran, Interpretation of signals from dropweight impact tests, Compos. Struct. 42 (4) (1998) 353–363.
[20] J. Lifshitz, F. Gov, M. Gandelsman, Instrumented low-velocity impact of CFRP beams, Int. J. Impact Eng 16 (2) (1995) 201–215.
[21] Shivakumar, K., W. Elber, and W. Illg, *Prediction of impact force and duration due to low-velocity impact on circular composite laminates.* 1985.
[22] P.J. Cain, Digital filtering of impact data, ASTM International, 1986.
[23] B. Sun, B. Gu, Frequency analysis of stress waves in testing 3-D angle-interlock woven composite at high strain rates, J. Compos. Mater. 41 (24) (2007) 2915–2938.
[24] M. Ohtsu, T. Isoda, Y. Tomoda, Acoustic emission techniques standardized for concrete structures, J. Acoust. Emission 2007 (25) (2007) 21–32.
[25] G. Michlmayr, D. Cohen, D. Or, Sources and characteristics of acoustic emissions from mechanically stressed geologic granular media—A review, Earth Sci. Rev. 112 (3–4) (2012) 97–114.
[26] R. Basavanna, S. Raja, Low Velocity Impact Response on GFRP and GF-SMP Panels in Structural and High Frequency Bands, Adv. Aeros. Sci. Technol. 5 (02) (2020) 58.
[27] S. Hoseinlaghab, et al., Tension-after-impact analysis and damage mechanism evaluation in laminated composites using AE monitoring, Mech. Syst. Sig. Process. 186 (2023), 109844.
[28] S. Do, B.R., N. Reed, A. Mohammed, K. Manlulu, G. Youssef, *Fabrication, characterization, and testing of novel polyurea foam.* Polyurethane Magazine, 2019. 16(2): p. 104-107.
[29] S. Do, et al., Partially-perforated self-reinforced polyurea foams, Appl. Sci. 10 (17) (2020) 5869.
[30] B. Koohbor, N. Pagliocca, G. Youssef, A multiscale experimental approach to characterize micro-to-macro transition length scale in polymer foams, Mech. Mater. (2021), 104006.
[31] K.Z. Uddin, et al., Gradient optimization of multi-layered density-graded foam laminates for footwear material design, J. Biomech. 109 (2020), 109950.

[32] G. Youssef, et al., Experimentally-validated predictions of impact response of polyurea foams using viscoelasticity based on bulk properties, Mech. Mater. 148 (2020), 103432.
[33] Gibson, L.J. and M.F. Ashby, *Cellular Solids: Structure and Properties*. 2 ed. Cambridge Solid State Science Series. 1997, Cambridge: Cambridge University Press.
[34] B. Koohbor, et al., Characterization of energy absorption and strain rate sensitivity of a novel elastomeric polyurea foam, Adv. Eng. Mater. 23 (1) (2021) 2000797.
[35] G. Youssef, Applied mechanics of polymers: properties, processing, and behavior, Elsevier, 2021.
[36] B. Ramirez, V. Gupta, Evaluation of novel temperature-stable viscoelastic polyurea foams as helmet liner materials, Mater. Des. 137 (2018) 298–304.
[37] B. Koohbor, et al., Dynamic Behavior and Impact Tolerance of Elastomeric Foams Subjected to Multiple Impact Conditions, J. Dynam. Behav. Mater. (2022) 1–12.
[38] B. Koohbor, N.K. Singh, A. Kidane, Radial and axial inertia stresses in high strain rate deformation of polymer foams, Int. J. Mech. Sci. 181 (2020), 105679.